

Supporting Information

Selenophenyl Bridged PeryleneDiimide Dimer as Efficient Solution-Processed Small Molecule Acceptor

Xin Zhang, Jiannian Yao, and Chuanlang Zhan*

Beijing National Laboratory of Molecular Science, CAS Key Laboratory of Photochemistry, Institute of Chemistry, Chinese Academy of Sciences, Beijing, P. R. China. E-mail: clzhan@iccas.ac.cn (C.Z.).

Contents

1. Experimental details.
 - (1) Methods and materials.
 - (2) Sample preparations.
 - (3) Quantum chemical calculations.
 - (4) Fabrications and characterizations of organic solar cell devices.
 - (5) Measurements of the hole mobility by the space-charge limited current (SCLC) method.
 - (6) Measurements of the electron mobility by the space-charge limited current (SCLC) method.
2. Synthesis.
3. Supporting figures.
 - (1) Figure S1. The ^1H NMR spectrum of **bis-PDI-Se-EG**.
 - (2) Figure S2. The ^{13}C NMR spectrum of **bis-PDI-Se-EG**.
 - (3) Figure S3. The optimal conformation of dimeric PDI **bis-PDI-Se-EG**.
 - (4) Figure S4. Cyclic voltammograms of **bis-PDI-Se-EG** in DCM with 0.1M Bu_4NPF_6 .
 - (5) Figure S5. $J-V$ curves of the best devices based on PBDTTT-C-T:**bis-PDI-Se-EG** with various contents of 1,8-diiodooctane (DIO).
 - (6) Figure S6. Plots of $\ln(JL^3/V^2)$ vs. $(V/L)^{0.5}$ obtained from the hole-only and electron-only device, which were estimated using the SCLC method.
4. Supporting tables.
 - (1) Summary of device performance for various BHJ devices based on P3HT:**bis-PDI-Se-EG** in the work.
 - (2) Summary of device performance for various BHJ devices based on PBDTTT-C-T:**bis-PDI-Se-EG** in the work.
5. References.

1. Experimental details.

1). Materials and Methods.

All reagents and chemicals were purchased from commercial sources (TCI, Acros, Sigma, or Alfa) and used without further purification except statements. Solvents (toluene and tetrahydrofuran) were distilled by standard procedures before used for organic synthesis. The polymer of PBDTTT-C-T ($M_n = 20000$ g/mol, PDI = ~3) was purchased from Solarmer company. The polymer of P3HT ($M_n = >50000$ g/mol, Regioregularity: 91%-94%) was purchased from Organtec Materials Inc..

^1H NMR and ^{13}C NMR spectra were recorded by a Bruker DMX-400 spectrometer with CDCl_3 as a solvent and tetramethylsilane as an internal reference. MALDI-TOF mass spectra using 4-chloro- α -cyanocinnamic acid (Cl-CCA) matrix were recorded by a Bruker BIFLEXIII. Elemental analysis was performed on a flash EA1112 analyzer. Transmission electron microscopy (TEM) tests were performed on a JEM-2100 operated at 200 kV. The TEM specimens were prepared by transferring the spin-coated films to the 200 mesh copper grids. All spectroscopic measurements were carried out at room temperature. The absorption spectrum was measured on Hitachi U-3010 UV-vis spectrophotometer. The solution spectrum was obtained using a 1 cm optical length quartz cell and the film spectrum was obtained via the transmission mode. The thickness of the solid films was measured by Dektak Profilometer. The electrochemical cyclic voltammetry (CV) was performed using a Zahner IM6e electrochemical work station in a 0.1 mol/L tetrabutylammoniumhexafluorophosphate (Bu_4NPF_6) dichloromethane (DCM) solution with a scan speed at 0.1 V/s. A Pt wire and Ag/AgCl were used as the counter and reference electrodes, respectively. The concentration of **bis-PDI-Se-EG** is adjusted as 1×10^{-4} mol/L in chromatographic pure DCM solution for the CV measurements.

2). Sample preparations.

Film samples for measurements of absorption spectrum and TEM are prepared via spin-coating method. The pure donor (D) films were spun-cast from an *o*-DCB solution of 20 mg/ml and the pure and acceptor (A) films were spin-coated from a chloroform solution of 10 mg/ml. All the blend films were prepared by spin-casting from an *o*-DCB solution of 40 mg/ml, in which both the donor and acceptor were mixed in a 1:1 weight ratio. For absorption spectrum, the *o*-DCB solution containing 1:1 (w/w) blended donor and acceptor was spin-coated onto PEDOT:PSS (Clevios P VP.AI 4083) layer, which was pre-coated on quartz substrate under the same conditions as those for preparation of a cell device. For TEM, the films were obtained by transferring the floated blend films from the water onto the Cu grid.

3). Quantum chemical calculations.

Density functional theory calculations were performed with the Gaussian 09 program,¹ using the B3LYP functional.² All-electron double- ξ valence basis sets with polarization functions 6-31G* were used for all atoms.³ Geometry optimizations were performed with full relaxation of all atoms in gas phase without solvent effects. Vibrational frequency calculations were performed to check that the stable structures had no imaginary frequency.

4). Fabrications and characterizations of organic solar cells.

Solar cell devices with a typical configuration of ITO/PEDOT: PSS/donor:acceptor/Ca/Al were fabricated as follows: The ITO glass was pre-cleaned with deionized water, CMOS grade acetone and isopropanol in turn for 15 min. The organic residues were further removed by treating with UV-ozone for 1 h. Then the ITO glass was modified by spin-coating PEDOT: PSS (poly(3,4-ethylenedioxythiophene)-poly(styrenesulfonate) layer, 30 nm) on it. After the ITO glasses were dried in oven at 150°C for 15 min, the active layer was spin-coated on the ITO/PEDOT:PSS using a blend solution of donor (P3HT or PBDTTT-C-T) and acceptor (**bis-PDI-Se-EG**) (40 mg/mL in *o*-dichlorobenzene, *o*-DCB), and optimized with different donor/acceptor weight ratio, different contents of DIO, and different thermal annealing temperature, respectively). Ca (20 nm) and Al (80 nm) electrode was then subsequently thermally evaporated on the active layer under the vacuum of 1×10^{-6} Torr. The active area of the device was 0.06 cm², and the thicknesses of the active films were ~90 nm. The devices were characterized in nitrogen atmosphere under the illumination of simulated AM 1.5 G, 100 mW/cm² using a xenon-lamp-based solar simulator (AAA grade, XES-70S1). The current-voltage (*I-V*) measurement of the devices was conducted on a computer-controlled Keithley 2400 Source Measure Unit. The EQE measurements were performed in air using QE-R3011 (Enli Technology Co. Ltd., Taiwan) with a scan increment of 10 nm per point.

5). Measurements of the hole mobility by the space-charge limited current (SCLC) method.

The devices were fabricated with configuration of ITO/PEDOT:PSS/donor:acceptor(200-250 nm)/Au. The Au layer was deposited under a low speed (1 Å/10 s) to avoid the penetration of Au atoms into the active layer. The active layers were spin-coated with *o*-DCB and dried. The hole mobility extracted by fitting the current density–voltage curves using the equation (1):⁴

$$J = 9/8 \epsilon \epsilon_0 \mu_h V^2 / L^3 \exp[0.89(V/E_0 L)^{0.5}] \quad (1)$$

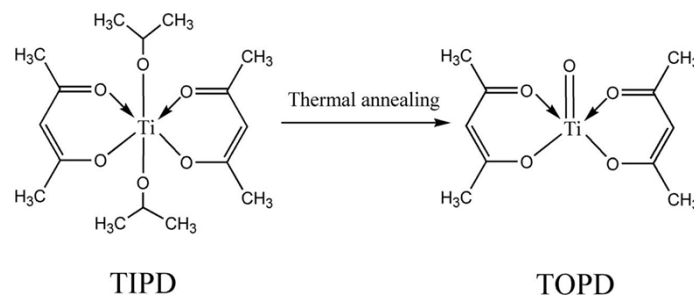
where ϵ is the dielectric constant of the polymer, ϵ_0 the permittivity of the vacuum, μ_h the zero-field mobility, E_0 the characteristic field, J the current density, L the thickness of the films, and $V = V_{\text{appl}} - V_{\text{bi}}$; V_{appl} is the applied

potential, and V_{bi} is the built-in potential which results from the difference in the work function of the anode and the cathode (in this device structure, $V_{bi}=0.2$ V). Herein ε is 3, ε_0 is 8.85419×10^{-12} CV⁻¹m⁻¹.

The results are shown in Figure S6. The hole mobility of the blending films were deduced from the intercept value of $\ln(9\varepsilon\varepsilon_0\mu_0/8)$ by linearly plotting $\ln(JL^3/V^2)$ vs $(V/L)^{0.5}$.

6). Measurements of the electron mobility by the space-charge limited current (SCLC) method.

The devices were fabricated with a configuration of ITO/titanium (diisopropoxide) bis(2,4-pentanedionate)⁵ (TIPD, 20nm)/donor:acceptor (150nm)/Al (1000nm). Since the HOMO and LUMO energy levels of the TIPD were -3.91 eV and -6.0 eV, it can be used to fabricate the electron-only SCLC device. The TIPD buffer layer was prepared by spin-coating a 3.5wt % TIPD isopropanol solution on the pre-cleaned ITO substrate and then baked at 150 °C for 10 min. Subsequently, the blended films were prepared using the same condition as the preparation of the best OSC device. Finally, the Allayer was thermally deposited on the top of the blended films in vacuum. Noted that TIPD is changed to TOPD after thermal annealing.⁵



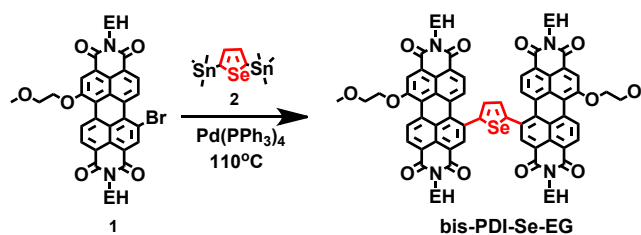
The electron mobilities were extracted by fitting the current density–voltage curves using the following equation (1):⁴

$$J=9/8\varepsilon\varepsilon_0\mu_e V^2/L^3 \exp[0.89(V/E_0L)^{0.5}] \quad (1)$$

where ε is the dielectric constant of the acceptor material, $\varepsilon_0=8.85419\times 10^{-12}$ CV⁻¹m⁻¹, μ_e the zero-field mobility, L the thickness of the films, and $V = V_{appl}-V_{bi}$; V_{appl} the applied potential, and V_{bi} the built-in potential which results from the difference in the work function of the anode and the cathode (in this device structure, $V_{bi} = 0$ V).

The results are shown in Figure S6. The electron mobility of the blending films was deduced from the intercept value of the plot of $\ln(JL^3/V^2)$ vs $(V/L)^{0.5}$.

2. Synthesis



Synthesis of compounds 2,5-bis(trimethylstannyl)selenophene (2).

A solution of *n*-BuLi (2.20 M in hexane, 1.00 mL, 2.20 mmol, 2.20 equiv) was added dropwise to a solution of selenophene (131.0 mg, 1.00 mmol, 1.00 equiv) in anhydrous THF (15 mL) in a Schlenk flask at -78 °C. After 1 h at -78 °C, the reaction mixture was stirred at ambient temperature for 30 min. Then, Me₃SnCl (1.00 M in THF, 2.50 mL, 2.50 mmol, 2.50 equiv) was added and the stirring was maintained for 1 h. After dilution with ethyl acetate (EtOAc, 50 mL), the mixture was washed with a saturated aqueous solution of KF (20 mL) and then water, dried over MgSO₄ and evaporated in vacuo leading to the crude product. 2,5-bis(trimethylstannyl)selenophene (**2**) (388.2 mg, 0.85 mmol, 85%) was recrystallized from methanol as a white crystal.

Synthesis of bis-PDI-Se-EG.

1 was synthesized according to the literature methods.⁶ A mixture of **1** (168.6 mg, 0.22 mmol) and 2,5-bis(trimethylstannyl)selenophene (**2**, 45.8 mg, 0.10 mmol) was dissolved in dry toluene (10 mL). A catalytic amount of Pd[P(C₆H₅)₃]₄ (6.94 mg, 0.006 mmol) was added and the reaction mixture was stirred at 110 °C for 36 h. The mixture was extracted with DCM and then washed with water. Then the DCM layer was dried over Na₂SO₄. After removal of DCM, the residue was subjected to chromatography with DCM/methanol (20:1) as eluents to afford the desired product **bis-PDI-Se-EG** (127.9 mg, 0.085 mmol, 85%) as a black solid; ¹H NMR (400MHz, CDCl₃) δ ppm: 9.62-9.45(m, 2H), 8.86-8.20 (m, 10H), 7.68-7.53 (m, 2H), 4.68-4.53 (m, 4H), 4.26-4.02 (m, 8H), 4.02-3.92 (m, 4H), 3.67-3.51 (m, 6H), 2.07-1.80 (m, 4H), 1.51-1.09 (m, 32H), 1.04-0.68 (m, 24H); ¹³C NMR (100MHz, CDCl₃) δ ppm: 164.4, 163.8, 163.6, 163.5, 157.4, 157.0, 146.9, 145.1, 135.2, 134.1, 133.4, 133.2, 132.3, 131.3, 130.1, 129.2, 128.9, 128.6, 128.4, 127.9, 127.6, 127.0, 123.8, 123.4, 122.4, 121.7, 121.4, 120.4, 117.6, 70.9, 69.4, 59.5, 44.5, 38.1, 31.0, 28.9, 24.3, 23.2, 14.3, 10.8; Elemental Analysis for C₉₀H₉₆N₄O₁₂Se: Calcd C, 71.94; H, 6.43; N, 3.72; Found C, 72.07; H, 6.42; N, 3.72. TOF MS: *m/z* = 1505.8 [M+H]⁺.

3. Supporting figures.

Figure S1. The ^1H NMR spectrum of **bis-PDI-Se-EG**.

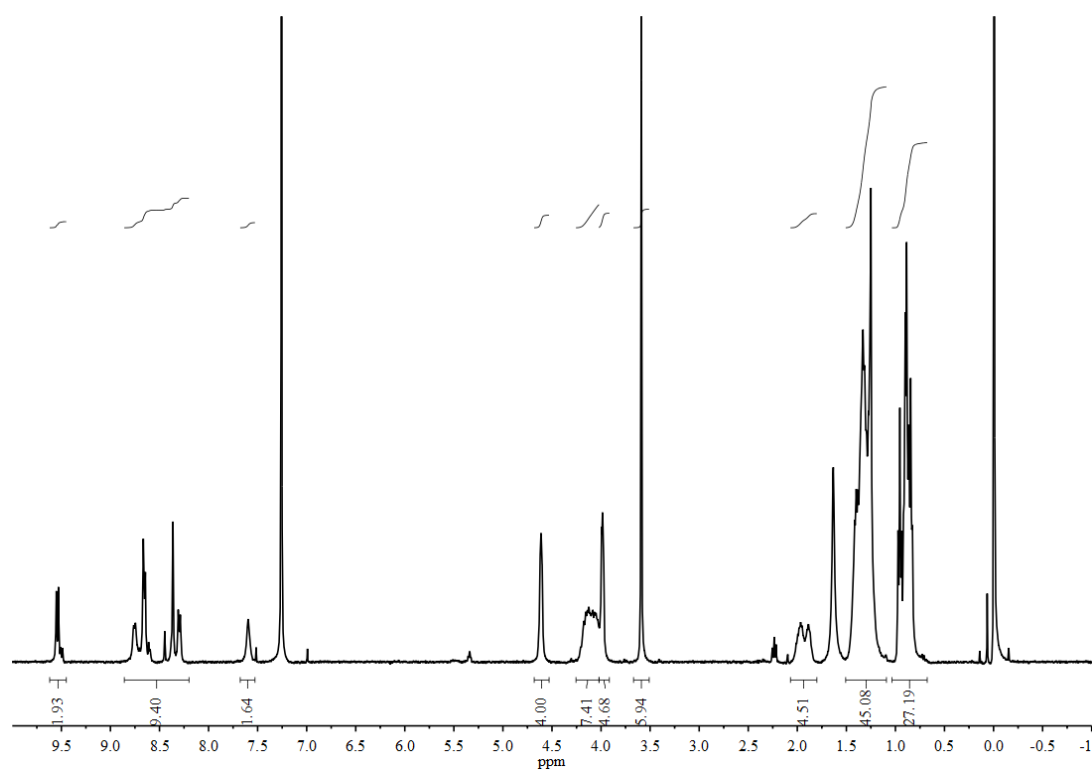


Figure S2. The ^{13}C NMR spectrum of **bis-PDI-Se-EG**.

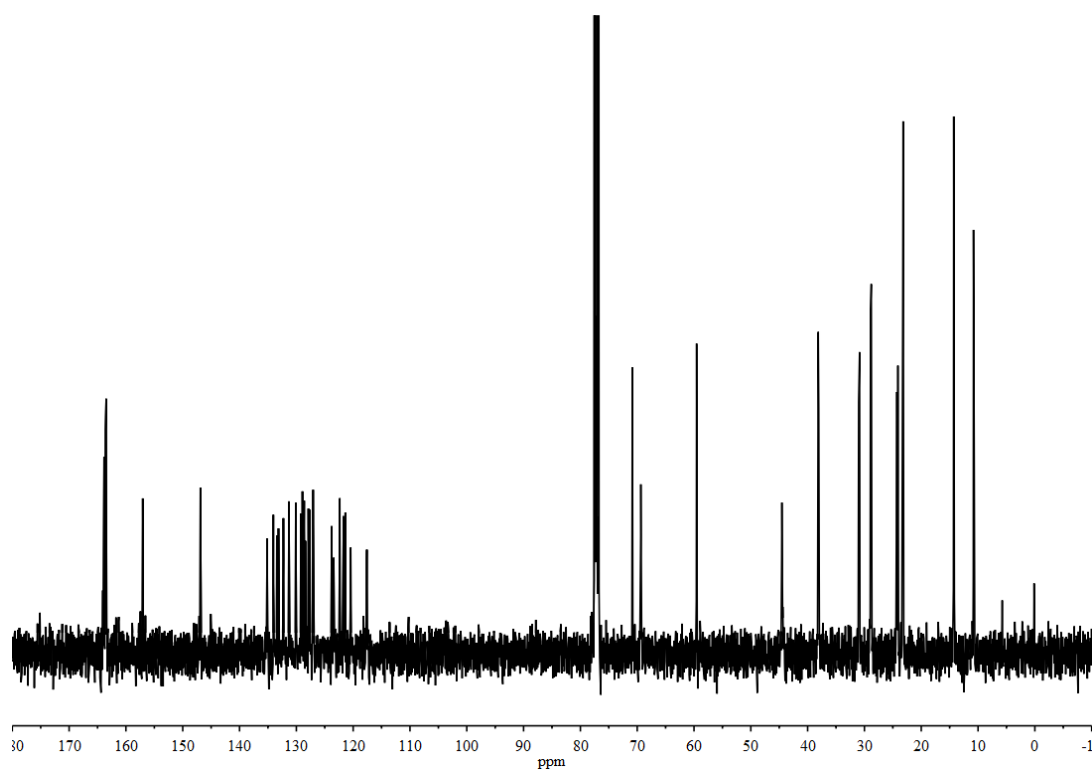
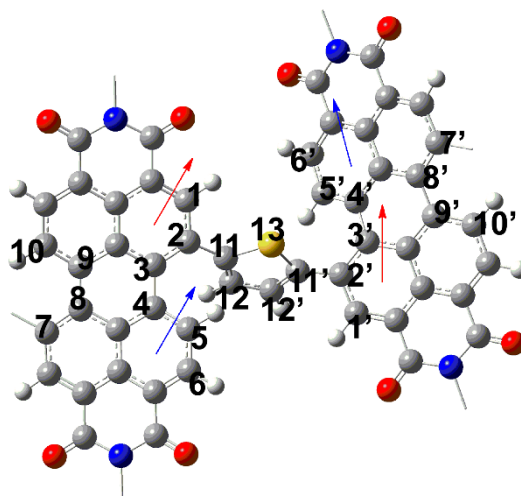


Figure S3. The optimal conformation of dimeric PDI of **bis-PDI-Se-EG** and the dihedral angles shown in the following table.



| | Atoms | Dihedral Angles (°) | | Atoms | Dihedral Angles (°) |
|--------------------------------|--------------|---------------------|------------------------------------|---------------|---------------------|
| PDI plane | 2-3-4-5 | 18.14 | PDI plane—selenophenyl plane | 1-2-11-12 | -120.52 |
| | 2'-3'-4'-5' | -19.87 | | 1-2-11-13 | 58.48 |
| | 7-8-9-10 | 14.74 | | 3-2-11-12 | 58.15 |
| | 7'-8'-9'-10' | -15.77 | | 3-2-11-13 | -124.84 |
| | av. | 19.01/15.26 | | 1'-2'-11'-13' | 123.84 |
| PDI—PDI planes ^a | | 25.20 | | 1'-2'-11'-12' | -55.38 |
| | | 18.58 | | 3'-2'-11'-13' | -52.90 |
| | av. | 21.89 | | 3'-2'-11'-12' | 127.88 |
| | | | | av. | 55.98 |

^aThe dihedral angle of PDI-PDI planes is calculated by intersection angle between the two normal vectors of PDI planes (Figure S3, red or blue arrows).

Figure S4. Cyclic voltammograms of **bis-PDI-Se-EG** in DCM with 0.1M Bu₄NPF₆. Scan rate was 100 mV s⁻¹, Ag/AgCl was used as reference electrode.

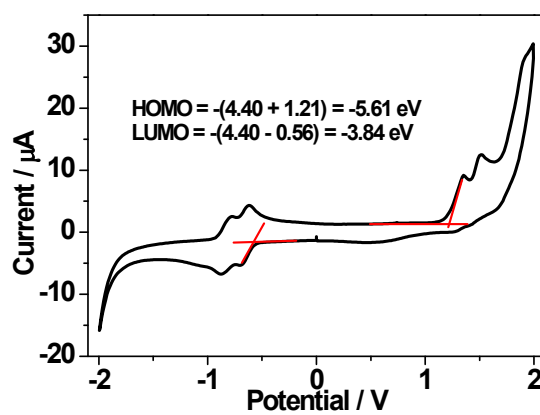


Figure S5. J - V curves of the best devices based on PBDTTT-C-T:bis-PDI-Se-EG with various contents of 1,8-diiodooctane (DIO). Note: The host solvent is *o*-DCB, D/A ratio = 1:1, solvent annealing (6h).

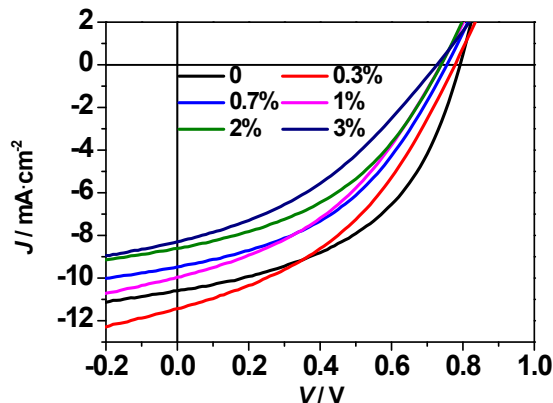
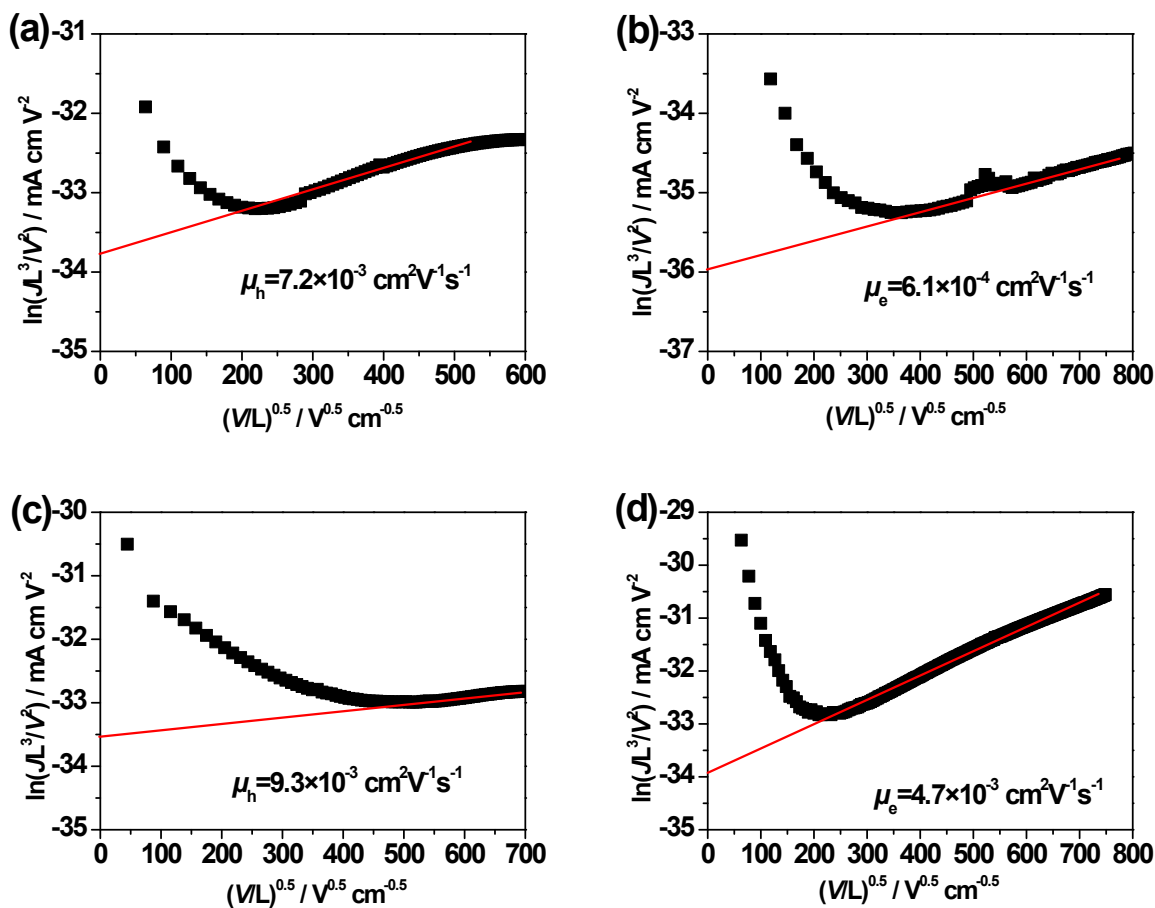


Figure S6. Plots of $\ln(JL^3/V^2)$ vs. $(V/L)^{0.5}$ obtained from the hole-only (a, c) and electron-only (b, d) device, which were estimated using the SCLC method. The devices based on P3HT:bis-PDI-Se-EG (a, b) and PBDTTT-C-T:bis-PDI-Se-EG (c, d) were fabricated under the optimal conditions respectively.



4. Supporting tables.

Table S1. Summary of device performance for various BHJ devices based on P3HT:**bis-PDI-Se-EG** in the work.

| Acceptor | D/A Ratio (w/w) | V_{oc} (V) | J_{sc} (mA/cm ²) | FF (%) | PCE (%) |
|---------------|--------------------|-----------------|-----------------------------------|-----------|------------|
| Bis-PDI-Se-EG | 1:1 ^a | 0.56 | 0.72 | 43.72 | 0.18 |
| | 1:1 ^b | 0.58 | 1.79 | 53.91 | 0.56 |
| | 1:1 ^c | 0.49 | 0.85 | 38.75 | 0.16 |
| | 1:2 ^b | 0.58 | 0.78 | 52.30 | 0.24 |
| | 1:1.5 ^b | 0.57 | 1.03 | 53.09 | 0.31 |
| | 1.5:1 ^b | 0.58 | 1.53 | 49.65 | 0.44 |
| | 2:1 ^b | 0.59 | 1.06 | 48.23 | 0.30 |
| | 1:1 ^{b,d} | 0.59 | 3.51 | 55.36 | 1.15 |
| | 1:1 ^{b,e} | 0.59 | 1.23 | 63.87 | 0.46 |
| | 1:1 ^{b,f} | 0.58 | 3.43 | 63.61 | 1.27 |
| | 1:1 ^{b,g} | 0.59 | 3.30 | 67.21 | 1.31 |
| | 1:1 ^{b,h} | 0.58 | 3.22 | 65.36 | 1.22 |

^achlorobenzene; ^b*o*-DCB; ^cchloroform; ^d solvent annealing; ^e thermal annealing (100 °C for 10 min); ^f solvent annealing and subsequent thermal annealing (100 °C for 10 min); ^g solvent annealing and subsequent thermal annealing (110 °C for 10 min); ^h solvent annealing and subsequent thermal annealing (120 °C for 10 min). Solvent annealing is conducted by using 5 μ L of *o*-DCB pre-added in a petri dish. The solvent annealing time is 4 h.

Table S2. Summary of device performance for various BHJ devices based on PBDTTT-C-T:**bis-PDI-Se-EG** in the work.^a

| | D/A Ratio (w/w) | DIO (%, v/v) | V_{oc} (V) | J_{sc} (mA/cm ²) | FF (%) | PCE (%) |
|---------------|--------------------|-----------------|-----------------|-----------------------------------|-----------|------------|
| Bis-PDI-Se-EG | 1:1.5 | 0 | 0.80 | 7.21 | 44.21 | 2.55 |
| | 1:1 | 0 | 0.79 | 10.60 | 47.93 | 4.01 |
| | 1.5:1 | 0 | 0.80 | 8.46 | 43.42 | 2.94 |
| | 1:1 | 0.3 | 0.78 | 11.44 | 40.72 | 3.63 |
| | 1:1 | 0.7 | 0.76 | 9.48 | 42.63 | 3.07 |
| | 1:1 | 1 | 0.74 | 9.96 | 40.02 | 2.95 |
| | 1:1 | 2 | 0.74 | 8.61 | 42.22 | 2.69 |
| | 1:1 | 3 | 0.73 | 8.30 | 36.95 | 2.24 |

^a *o*-DCB, solvent annealing (6h).

References:

- (1) Frisch, M. J.; Trucks, G. W.; Schlegel, H. B.; Scuseria, G. E.; Robb, M. A.; Cheeseman, J. R.; Scalmani, G.; Barone, V.; Mennucci, B.; Petersson, G. A.; Nakatsuji, H.; Caricato, M.; Li, X.; Hratchian, H. P.; Izmaylov, A. F.; Bloino, J.; Zheng, G.; Sonnenberg, J. L.; Hada, M.; Ehara, M.; Toyota, K.; Fukuda, R.; Hasegawa, J.; Ishida, M.; Nakajima, T.; Honda, Y.; Kitao, O.; Nakai, H.; Vreven, T.; Montgomery, J. A., Jr.; Peralta, J. E.; Ogliaro, F.; Bearpark, M.; Heyd, J. J.; Brothers, E.; Kudin, K. N.; Staroverov, V. N.; Kobayashi, R.; Normand, J.; Raghavachari, K.; Rendell, A.; Burant, J. C.; Iyengar, S. S.; Tomasi, J.; Cossi, M.; Rega, N.; Millam, J. M.; Klene, M.; Knox, J. E.; Cross, J. B.; Bakken, V.; Adamo, C.; Jaramillo, J.; Gomperts, R.; Stratmann, R. E.; Yazyev, O.; Austin, A. J.; Cammi, R.; Pomelli, C.; Ochterski, J. W.; Martin, R. L.; Morokuma, K.; Zakrzewski, V. G.; Voth, G. A.; Salvador, P.; Dannenberg, J. J.; Dapprich, S.; Daniels, A. D.; Farkas, Ö.; Foresman, J. B.; Ortiz, J. V.; Cioslowski, J.; Fox, D. J. Gaussian 09, Revision A.02, Gaussian, Inc., Wallingford CT, 2009.
- (2) (a) Lee, C. T.; Yang, W. T.; Parr, R. G. *Phys. Rev. B* **1988**, *37*, 785; (b) Becke, A. D. *J. Chem. Phys.* **1993**, *98*, 5648.
- (3) Krishnan, R.; Binkley, J. S.; Seeger, R.; Pople, J. A. *J. Chem. Phys.* **1980**, *72*, 650.
- (4) (a) Mott, N. F.; Gurney, D. *Electronic Processes in Ionic Crystals*, Academic Press, New York **1970**, p. 45; (b) Murgatroyd, P. N. *J. Phys. D: Appl. Phys.* **1970**, *3*, 151; (c) Campbell, A. J.; Bradley, D. D. C.; Lidzey, D. G. *J. Appl. Phys.* **1997**, *82*, 6326; (d) Malliaras, G. G.; Salem, J. R.; Brock, P. J.; Scott, C. *Phys. Rev. B* **1998**, *58*, 13411; (e) An, Z.; Yu, J.; Jones, S. C.; Barlow, S.; Yoo, S.; Domercq, B.; Prins, P.; Siebbeles, L. D. A.; Kippelen, B.; Marder, S. R. *Adv. Mater.* **2005**, *17*, 2580.
- (5) Tan, Z. A.; Zhang, W. Q.; Zhang, Z. G.; Qian, D. P.; Huang, Y.; Hou, J. H.; Li, Y. F. *Adv. Mater.* **2012**, *24*, 1476.
- (6) Zhang, X.; Pang, S. F.; Zhang, Z. G.; Ding, X. L.; Zhang, S. L.; He, S. G.; Zhan, C. L. *Tetrahedron Lett.* **2012**, *53*, 1094.